Coventry University and
The University of Wisconsin Milwaukee Centre for By-products Utilization,
Second International Conference on Sustainable Construction Materials and Technologies
June 28 - June 30, 2010, Università Politecnica delle Marche, Ancona, Italy.
Web only Papers. http://www.claisse.info/Proceedings.htm

Easy assessment of durability indicators for concretes with high volume of SCMs

V. Baroghel-Bouny [1*], K. Kinomura[1,2], M. Thiery[1], S. Moscardelli[3]

[1] *Paris Est Univ., Laboratoire Central des Ponts et Chaussées (LCPC), Paris, France, e-mail: baroghel@lcpc.fr*
[2] *Taisei Corporation, Tokyo, Japan*
[3] *Laboratoire Régional des Ponts et Chaussées de l'Est Parisien (LREP), Le Bourget, France*

ABSTRACT

In recent years, sustainable development has become a major concern, in particular in the construction field. In this context, a global approach is needed, in order to meet technical, economical, environmental and societal requirements in an optimized way for the whole life cycle of a concrete structure. In particular, it is needed to combine improved durability and environmentally friendly materials and structures. The recent development of performance-based approaches makes this now easier. In this paper, it is investigated if durability indicators (DIs), which are basic tools with regard to durability, more specifically transport properties, can be assessed by simple and rapid methods, e.g. direct experimental methods or indirect methods based on analytical formulas, for every type of concretes. Thus, first the results obtained by direct measurement on a broad range of materials particularly on high-volume SCM mixtures of electrical resistivity and *apparent* chloride diffusion coefficient are discussed. Then, various methods, in particular methods based on these parameters, are compared for the assessment of *effective* chloride diffusion coefficient and liquid water permeability, including in this last case a sophisticated method based on numerical inverse analysis. The very good agreement observed between the various methods points out that simple and rapid methods can allow assessment of DIs with sufficient accuracy. Moreover, a database, which includes values of electrical resistivity, *effective* and *apparent* chloride diffusion coefficients, and liquid water permeability, is available. Furthermore, the specificities of mixtures with high volume of SCMs have been highlighted.

INTRODUCTION

In recent years, sustainable development has become a major concern, in particular in the construction field [1,2]. In this context, a global approach is needed, in order to meet technical, economical, environmental and societal requirements in an optimized way for the whole life cycle of a concrete structure [3,4]. The job of designers, engineers and structure owners is therefore now more complex. In particular, they need to combine improved durability and environmentally friendly materials and structures. From a material point of view, they are thus interested, on the one hand in relevant parameters, which can characterize durability, and on the other hand in the use of wastes, by-products or recycled materials, which are, at least at the present time, regarded as zero-CO_2 emission constituents. As a consequence and in order to make this job easier, there is an increasing demand to include in current concrete or design standards advanced concepts of durability and service life (SL)

prediction, such as performance-based and/or probabilistic approaches, in particular with respect to the prevention of steel corrosion in reinforced concrete (RC) structures [5,6].

In this context, a general approach based on so-called *durability indicators* (DIs), which are key material properties with regard to durability, has been developed [3,7,8]. A system of classes of "potential" durability with respect to reinforcement corrosion has been proposed for each *DI*. These five classes - very low (VL), low (L), medium (M), high (H) and very high (VH) "potential" durability - can be used for example for mixture comparison or quality control. The evaluation of the "potential" durability of a given RC will consist in comparing the values of the measured DIs to the limits of the associated classes. Another purpose of this approach is to design concrete mixtures capable of protecting structures against degradation for given target structural service life (SL) and environmental conditions, thanks to performance-based criteria (specifications) related to the DIs. Furthermore, a multi-level modelling concept has been developed for SL prediction [8,9]. It can be applied to predict the SL of a given new structure at the design stage or the "residual" lifetime of an existing and possibly deteriorated structure. Since the concrete composition, which is often lacking for existing structures, is not needed, this approach can be very easily applied to them, in view of monitoring, diagnosis, maintenance and support to serviceability extension or repair decision. Note that this is the same DI set, which is involved in the classes, specifications and as input data for the models of SL prediction.

Consequently, it is of importance to:

- investigate if these DIs can be assessed by simple and rapid methods, in order to easily include them in a more general set of (sustainability) indicators and in harmonized standard methodologies,
- focus on materials with local aggregates and with high volume of supplementary cementing materials (SCMs) such as fly ash (FA) or ground granulated blast furnace slag (GGBS).

It is well known that the properties of a given type of SCM can be very variable (e.g. major effects of the specific surface area, alkalinity and glass content) and that a complete characterization of SCMs can be very complex [10]. As a consequence, for example some properties found for one FA cannot be generalized to all the FA. However, it is possible to take benefit of the numerous researches carried out worldwide for a long time in particular in North America on these materials (see e.g. [11-14]).

Hence, this paper will focus on the assessment of DIs, more specifically of the transport properties *effective* chloride diffusion coefficient and liquid water permeability, by various methods, on a broad range of materials including mortars or concretes with FA as well as CEM-III concretes. The range of SCM contents has been selected to be relevant from a practical point of view or to be that commonly used in concretes. The purpose here is to validate the use of simple and rapid methods (e.g. direct experimental methods or indirect methods based on analytical formulas) and to check their applicability particularly to high-volume SCM mixtures. Comparison with a more sophisticated method based on numerical inverse analysis will be carried out for liquid water permeability. Another aim here is to provide a database, not only for transport properties (*apparent* and *effective* chloride diffusion coefficients, as well as liquid water permeability) but also for electrical resistivity, able to give an idea of the values expected for these DIs and their corresponding classes, within the framework of the associated performance-based approach. Moreover, the specificities of high-volume SCM mixtures will be pointed out.

MATERIALS AND EXPERIMENTS

Materials. A broad range of concretes, ranging from low-grade materials (average 28-day cylinder compressive strength, c.s., around 20 MPa) up to very-high-performance concretes (28-day c.s. > 90 MPa), has been tested in lab conditions at T = 21 ± 1 °C. The mix-composition and the average 28-day cylinder c.s. of some of the concretes investigated in the paper are reported in Table 1. Various CEM I and CEM III have been used and the water-to-binder ratio (W/B) ranges from 0.23 to 0.84. The composition of the CEM I used for the "M" series [15] (see Table 1) and for several other concretes is given in [16]. With regard to CEM III/A, the GGBS content is 43% (LR59-1-III) or 62% (e.g. BO-III and LR77-3-III) per unit mass of binder. In order to complement the data, one CEM III/C concrete with 85% GGBS has been tested (denoted B30-III/C). Air-entraining admixture (AEA), fly ash or silica fume (SF) were incorporated in some of the mixtures. In the materials with AEA, the air content of the fresh concrete ranges from 2 to 8%. The SF content ranges from 6% to 11% per unit mass of binder. In the FA-concretes, the FA content is 20% (M25FA, M25FA-EA, M50FA and M50FA-EA), 30% (M30FA), 35% (CFA) or 39% (B50FA) per unit mass of binder. The FA used for the various materials is the same (its composition is given in [16] and its specific surface area is 1.73 $m^2.g^{-1}$), except for concretes CFA [7] and B50FA. Not only lab mixtures, but also mixtures commonly used in bridges in various locations in France and in neighbouring countries (which include in particular local aggregates) have been studied (e.g. mixtures denoted "LR", such as LR77-3-III, which is considered suitable for exposure class XA2, or LR59-2, for exposure class XS3, according to EN 206-1).

Table 1. Mix-composition and average 28-day cylinder c.s. of some of the tested concretes

Concrete	CFA	BO-VB	M25	M30FA	M50	M75SF	LR59-1-III	LR77-3-III	BO-III
Cement	1 (CEM I 42.5)	2 (CEM I 52.5)	3 (CEM I 52.5)				4 (CEM III/A 42.5)	5 (CEM III/A 52.5)	6 (CEM III/A 42.5)
Gravel (G) content ($kg.m^{-3}$) (min/max grain size in mm)	949 (6/16)	1192 (4/20)	1007 (5/20)	986 (4/20)	937 (5/20)	1044 (5/20)	980 (4/20)	930 (6.3/20)	1036 (6.3/20)
Sand (S) content ($kg.m^{-3}$) (min/max grain size in mm)	911 (0/5)	744 (0/5)	899 (0/5)	879 (0/5)	806 (0/5)	877 (0/5)	890 (0/4)	800 (0/4)	715 (0/4)
Cement (C) content ($kg.m^{-3}$)	260	353	230	223	410	360	385	400	342
Fly ash (FA) content ($kg.m^{-3}$)	140			95					
Silica fume (SF) content ($kg.m^{-3}$)						22			
Water (W) content ($kg.m^{-3}$)	193	172	193	166	197	136	159	195(2)	186
Plasticizer or superplasticizer content ($kg.m^{-3}$)	4.8			1.1		12.0	1.14	1.20	
Retarder content ($kg.m^{-3}$)				1.4		2.5			
Water-to-cement ratio (W/C)	0.74	0.49	0.84	0.74	0.48	0.38			
Water-to-binder ratio (W/B)	0.48	0.49	0.84	0.52	0.48	0.36	0.41	0.49(*)	0.54
SCM-to-binder ratio				0.30		0.06	0.43	0.62	0.62
Gravel-to-sand ratio (G/S)	1.0	1.6	1.1	1.1	1.2	1.2	1.1	1.2	1.4
Average 28-day cylinder compressive strength (MPa)	28.9	49.5	25.1	48.5	55.5	85.5	75.5	41.0	38.5

(*): efficient water

Moreover, in order to understand more precisely the FA effect, mortars with various FA contents (0, 10, 20 and 30% per unit mass of binder), denoted FA-0, FA-10, FA-20 and FA-30 respectively, and with a high amount of limestone filler (60% per unit mass of binder, mainly to improve the properties of the fresh material) have also been studied. The mass amount of binder or of powder materials, as well as W/B, are the same for all the mortars (binder content = 511 $kg.m^{-3}$, W/powder = 0.28, and W/B = 0.45). Same ingredients (cement, FA, and sand) as for the "M" concrete series, and in particular M30FA, have been used. The

amount of admixtures was selected to comply with the proper rheology properties of high-fluidity mortars. FA-30 is regarded in Japan, within the framework of underground disposal facilities for radioactive wastes with multicomplex artificial barriers, as a basic mortar mixture expected to prevent for very long term diffusion of nuclide molecules emitted from radioactive wastes [17]. Note that the possible synergic effects between FA and limestone filler (e.g. acceleration of early hydration and formation of carboaluminate by limestone, and later strength development and microstructure densification by fly ash pozzolanicity), likely to enhance mechanical strength and durability, will not be considered in this paper.

Experiments. Electrical resistivity measurements, steady-state (ss) and non-steady-state (nss) migration tests, nss diffusion tests, as well as drying experiments, have been carried out. The test procedures are detailed in the following sections. In addition, the porosity accessible to water (Φ) has been measured by means of hydrostatic weighing, and mercury intrusion porosimetry (MIP) tests have been performed to complement the analysis (assessment of porosity P_{Hg}, pore size distribution and critical diameter d_c). The test methods are described in [18]. The MIP device used here allows one to investigate pores whose radius ranges from 1.8 nm to 60 μm ($P_{max.}$ = 400 MPa), except in some cases, which will be indicated in the paper, where $P_{max.}$ = 200 MPa and where consequently the pore radii range from 3.7 nm to 60 μm. "Representative" specimens (several pieces of approximately 1 cm^3 each) were prepared for MIP tests, by excluding however the coarser pieces of aggregates. Prior to measurement, the specimens were oven dried for 14 days under vacuum at T = 45 ± 1 °C in the presence of silica gel, or freeze-dried [18].

ELECTRICAL RESISTIVITY

Significance. Since electrical current is carried mainly *via* the liquid phase (by ions), the pore network connectivity of water saturated hardened cementitious materials can be characterized indirectly by measuring the electrical resistivity (being the inverse of conductivity σ) [19]. The electrical resistivity (ρ') can be measured on lab samples or can be used *in situ* as a non-destructive test for monitoring the durability of structures [20]. Some authors suggested hence that a resistivity test could be used for the control of the production of concretes with pre-defined durability requirements and even for concrete acceptance purposes (see e.g. [21,22]). In addition, the *effective* chloride diffusion coefficient could be calculated from a sole resistivity measurement (see next sections and [19,22,23]). Moreover, durability specifications (acceptance threshold values) can be based on this parameter [7], and models involving electrical resistivity have also been developed [19,22] for SL prediction, which include both the initiation and propagation periods according to *Tuutti's* definition [24].

Test method. The technique used here to measure electrical resistivity is described in [25] (see also [21] or [22]). The resistivity test is a simple, quick, cheap and non-destructive method, which however requires some carefulness [26]. It consists in placing a pair of stainless steel electrodes on the parallel surfaces of a saturated sample and measuring the alternating current I induced by the application of a potential drop ΔE (10 V or lower). The electrical contact is ensured by two wet sponges. ρ' is then calculated by geometrical conversion according to *Ohm's* law (see Eq. (1)):

$$\rho' = \frac{\Delta E}{I} \cdot \frac{A}{e} \qquad (1)$$

where A is the cross sectional area of the electrodes (*i.e.* of the sample) and e is the distance between electrodes (*i.e.* the height of the sample).

It can be deduced from the literature that the reproducibility coefficient of variation (COV) is 9-30% (see e.g. [20,27,28]) and the repeatability COV is 11% [27].

Results and discussion. ρ' has been measured here on a broad range of water-cured and water-saturated materials at various ages. Fig. 1 displays the experimental results (average values of three samples) plotted *vs.* the average 28-day cylinder c.s.. The classes of "potential" durability with respect to reinforcement corrosion (VL, L, M and H, see introduction) are also reported in the graph (the associated thresholds are 50, 100, 250 and 1000 Ω.m [7]). Fig. 2 displays the experimental results obtained for the mortars (W/B = 0.45).

In the general case, ρ' depends on porosity and also on the tortuosity and connectivity of the pore system, on the conductivity of the pore solution (σ_0), on the surface conductivity of the pore walls (adsorption of elements from the pore solution on C-S-H gel), and on the volume of aggregates, ...

The effect of pozzolanic materials (FA or SF) on pore structure, and thus on transport properties, is not only a "filler" effect (more significant with SF, which size is 100 times smaller than that of FA), but is also the result of chemical reactions. Note that the presence of fine particles can also induce acceleration of hydration reactions of the cement (nucleation sites for $Ca(OH)_2$ and C-S-H precipitation) and therefore earlier densification of the microstructure [29]. $Ca(OH)_2$ crystals are consumed by pozzolanic reaction, while finely divided C-S-H hydrate gel is formed, thus yielding a denser microstructure. In addition, when the FA (or slag) content increases, fibril-type C-S-H are progressively replaced by foil-type ones, which are more efficient to fill capillary pores [30]. Moreover, additional C-S-H (or other gel-type hydrate) form mainly far from the initial cement grains and from pseudoform C-S-H [31]. These additional C-S-H thus create solid islands, between partially reacted grains or pre-existing hydrate clusters, which increase the pore network tortuosity (pore blocking within the range involved in chloride ion transport). However, this physical effect induced by chemical reactions will be efficient only once the pozzolanic reaction has significantly progressed, which means in the case of FA far later after hydration (or pozzolanic reaction with SF [29]) has started (e.g. several months) [3,32]. In addition, this effect depends on the $Ca(OH)_2$ amount initially available, which has been formed by hydration of the portland cement and which can be affected by early-age drying or carbonation [3,32]. Likewise, hydration of the latent hydraulic GGBS requires a sufficient quantity of $Ca(OH)_2$ released by hydration of the portland cement, and the C-S-H formed (in the case of alkaline activation) are denser than that formed with portland cement while their C/S is lower (closer to 1) [30].

Moreover, the presence of SCMs changes the concentration and the mobility of the ions in the pore solution (e.g. as a result of modifications of the electrical double-layer at the solid-liquid interface [31,33-35]). For example, the presence of SF induces a significant decrease in alkali and hydroxyl ions in the pore solution [36,37], and according to [38], when 30% of the cement is replaced by FA, the concentration of hydroxyl ions is also reduced (see also [31]). Since the conductivity of the pore solution σ_0 can be estimated from the contribution of the Na^+, K^+ and OH^- alone, σ_0 will decrease and so the conductivity of the porous material σ (σ is proportional to σ_0 [39]). This will induce an increase in ρ'.

As a consequence of the various effects mentioned, Fig. 1 shows that the presence of FA, GGBS or SF induces high resistivity values. For example, according to the values reported in Fig. 1, HPCs with SF display values between 380 and 670 Ω.m, thus indicating a high "potential" durability. Fig. 3a displays MIP results obtained on concretes B80-2 and B80SF-S according to the procedure described in a previous section (after 14-day oven drying at T = 45±1 °C under vacuum and with silica gel). This figure confirms that the marked difference recorded on ρ' between HPCs with and without SF, for a same c.s., here ≈ 76 MPa (and even

for a similar MIP porosity, here ≈ 7.5%, see Fig. 3a), results, in addition to the changes in the pore solution, from the drastic refinement of the pore structure. Concretes with a high content of fly ash (between 30% and 39% per unit mass of binder) display values between 110 and 465 Ω.m, depending on the age, which mean medium or high "potential" durability. CEM III/A concretes (with 43% or 62% GGBS per unit mass of binder) display values between 230 and 595 Ω.m, depending on the age, which mean likewise medium or high "potential" durability. In the case of CEM III/C with 85% GGBS, the value recorded at the age of 3 years reaches 945 Ω.m (high "potential" durability).

In Fig. 1 the different values circled for a same c.s denote the results obtained for a same concrete at various ages (e.g. BO-III: 28 days, 90 days, 1 year and 2 years) and point out the significant resistivity increase with the age for FA- or CEM-III/A- concretes. Likewise, Fig. 2 shows the increase in the resistivity of the mortars with the age and with the FA content. This is the result of the microstructural changes previously mentioned, induced by hydration in all cases and by pozzolanic reaction in the case of FA materials. This increase is well correlated with the evolution of the MIP pore size distribution (see Fig. 4 for FA-materials and [3,17,32]). The resistivity of plain OPC - CEM I materials also increases with the age but in a lesser extent (see Fig. 1), as already reported in the literature (see e.g. [40]).

As illustrated in Fig. 2, when the pozzolanic reaction with fly ash has not progressed very much (age = 90 days), the ρ' values are very similar in the case of 0, 10, 20 and 30% FA. In particular, the difference between FA-0 and FA-10 becomes significant only at 180 days. The (slight) difference, which is recorded between the cases 20-30% FA and 0-10% FA at 90 days, can be explained by the decrease in the connectivity induced by the filler effect associated with the presence of 20-30% FA, a slight pozzolanic effect, the acceleration of hydration and therefore of the densification of the microstructure, or the decrease in the concentrations of some ions in the pore solution in the presence of FA (see above). Nevertheless, the similarity of the ρ' values at 90 days for the various FA contents indicates that this last effect does not significantly affect the measurement. Therefore, comparison between materials with and without FA by using the resistivity parameter is quite valid and the difference recorded at later ages can mainly be explained by changes in the pore structure (refinement). These findings tend to confirm that electrical resistivity is a good indicator of the connectivity of the pore network for both OPC and FA concretes. Nevertheless, the analysis is easy in the case of the mortars studied here, since the various mixtures have same constituents.

With regard to plain OPC - CEM I mixtures, ranging from 25 MPa (M25, W/C = 0.84, see Table 1) to 86 MPa (LR59-2, W/C = 0.38), the ρ' values range from 60 to 145 Ω.m between 28 days and 1 year, therefore displaying low or medium "potential" durability (see Fig. 1). These values are in agreement with the data reported in the literature (e.g. 50-200 Ω.m in [20]).

For a given type of binder (e.g. CEM I, CEM I + SF, CEM I + FA or CEM III/A), the electrical resistivity does not depend a lot on the 28-day c.s. (in particular on the W/B): the range of ρ' values measured is small even if the range of 28-day c.s. is very large, compared to the variation induced on the ρ' value when changing the binder at a given 28-day c.s. (see Fig. 1). Therefore, for example in the case of plain OPC - CEM I mixtures, within a broad 28-day c.s. range, resistivity measurement does not seem very discriminating, in particular when the data are compared to values obtained with FA-, GGBS- or SF-concretes (see Fig. 1). This can be explained first by the fact that the pore system connectivity can be more drastically changed by including SCM than by keeping CEM I and changing W/C (e.g.

between 0.35 and 0.50) (see Fig. 3b). Likewise, slight changes are recorded in the MIP pore size distribution of 62%-GGBS CEM III/A concretes when changing W/B (e.g. 0.44 and 0.54) (see Fig. 3b). In addition, it has been reported in the literature that, for plain OPC - CEM I materials, when W/C increases (in particular for W/C $\geq$ 0.50), ionic concentrations decrease in the pore solution and consequently σ_0 decreases [41,42]. This will induce an increase in ρ', which counteracts the decrease induced by the higher pore network connectivity. Note that the (overall) ρ' value measured in this case does not reflect mainly the connectivity of the pore system and cannot be directly compared to the values obtained for other types of materials.

According to the results presented in Fig. 1, no systematic effect of AEA is observed on ρ'.

It can be concluded that electrical resistivity measurement is an easy method to characterize the connectivity of the pore system, also for high-volume SCM mixtures. However, in particular the ionic composition of the pore solution (which depends on the composition of binder and aggregates, and of W/C) can significantly affect the (overall) ρ' value measured in the case of high-porosity plain OPC - CEM I concretes [25]. As a consequence, electrical resistivity is more appropriate to distinguish the binder, in particular the presence and the amount of SCM, compared to plain OPC - CEM I concretes, than to distinguish (and rank) various CEM I (or CEM III/A) concretes. It seems hence difficult to provide a single ranking based on resistivity for a whole set of concretes.

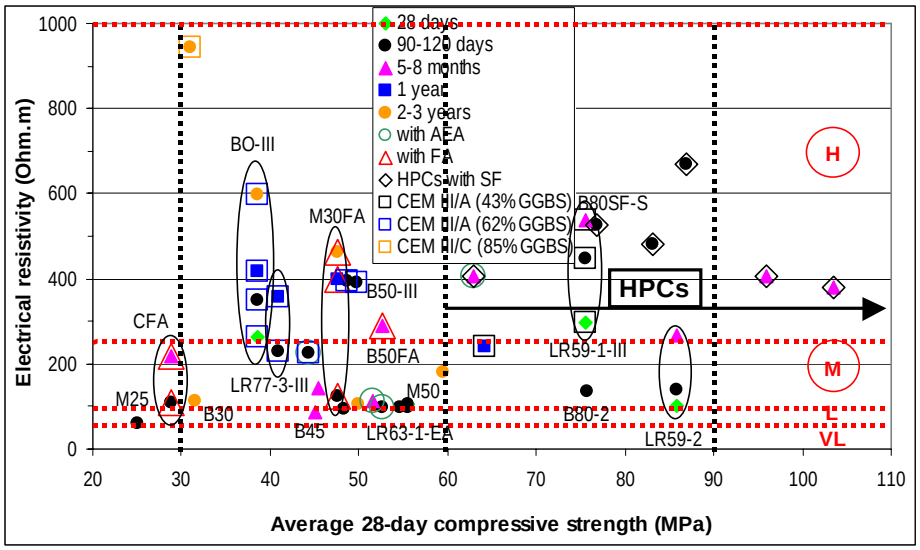

Fig. 1: "Potential" durability classes and experimental mean values of electrical resistivity measured on various water-cured and water-saturated concrete samples *vs*. the average 28-day cylinder c.s..

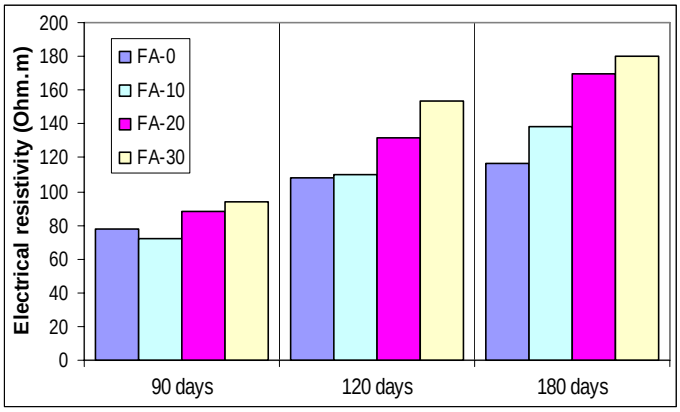

Fig. 2: Experimental mean values of electrical resistivity measured on water-cured and water-saturated mortar samples (W/B = 0.45) with various FA-contents, as a function of the age.

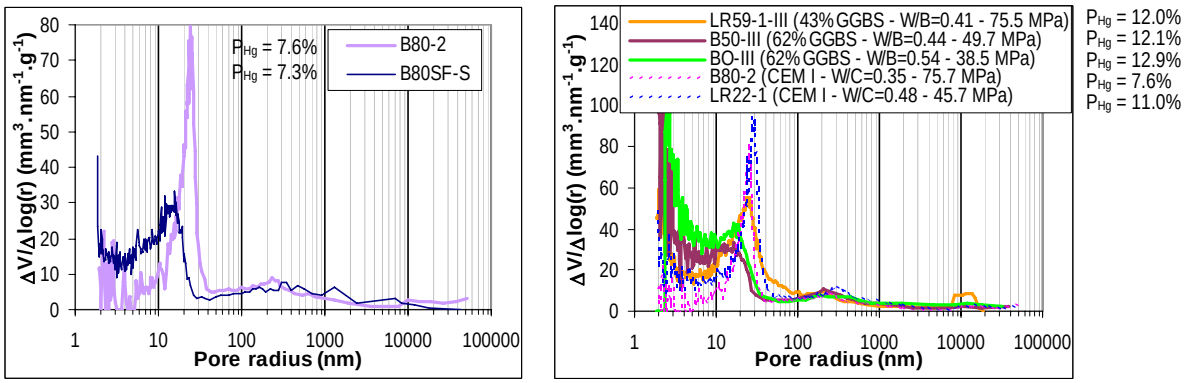

a) concretes B80-2 (SF/C = 0) and B80SF-S (SF/C = 0.08), with W/C = 0.35 and same CEM I 52.5 as the "M" series

b) CEM III/A concretes. Comparison with CEM I concretes

Fig. 3: MIP pore size distributions measured in concretes samples at 90 days after water curing and 14-day oven drying at T = 45±1 °C under vacuum and with silica gel.

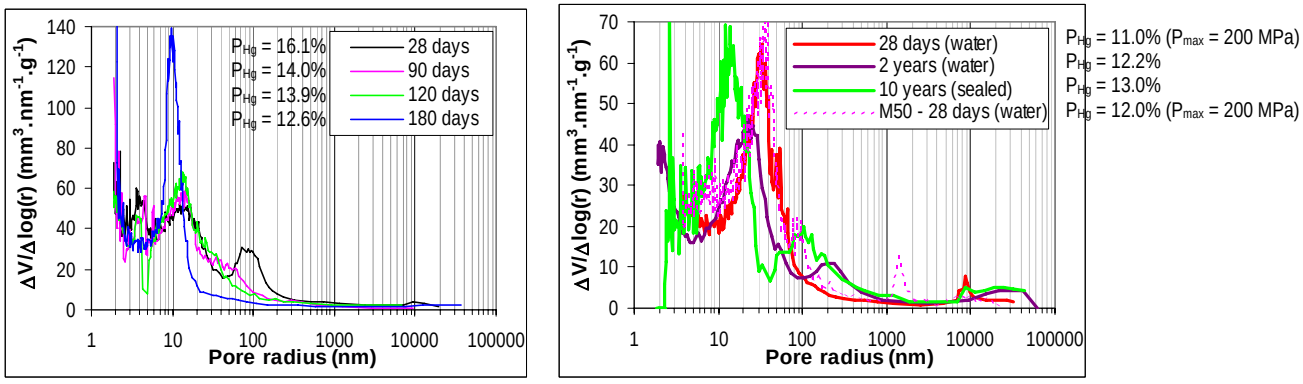

a) mortar FA-30 after 28-, 90-, 120- and 180-day water curing in lab (and freeze drying)

b) concrete M30FA after 28-day and 2-year water curing and after 10-year sealed curing in lab (and 14-day oven drying at T = 45 ± 1°C under vacuum and with silica gel). Comparison with M50 at 28 days

Fig. 4: MIP pore size distributions of 30%-FA materials after various curing conditions in lab.

APPARENT CHLORIDE DIFFUSION COEFFICIENT

Direct assessment of the *apparent* chloride diffusion coefficient $D_{ns(mig)}$ from nss migration test. The colorimetric measurement ($AgNO_3$ spray test) of the average chloride penetration depth (x_d), after a nss migration test under an external electrical field, allows, with several assumptions [43], the easy and rapid assessment of an *apparent* chloride diffusion coefficient $D_{ns(mig)}$ by applying the modified *Nernst-Planck* equation. As a matter of fact, in saturated conditions, the advection flow term of this equation can be neglected. In addition, when the electrical field $\Delta E/e$ is large enough and the penetration depth x_d is sufficient ($x_d > (\Delta E/e)\cdot(ZF/RT)\cdot D_{ns(mig)}\cdot t$), the diffusion term of the equation can also be neglected with respect to the electrical migration one [44]. Moreover, activity effects and interactions between ions can be neglected by assuming very dilute solutions and chlorides as the single species in the pore solution, respectively. Hence, $D_{ns(mig)}$ can be calculated by the following widely used solution proposed by *Tang and Nilsson* [45] (see Eq. (2)):

$$D_{ns(mig)} = \frac{R.T}{Z.F}\cdot\frac{e}{\Delta E}\cdot\frac{x_d - \alpha\cdot\sqrt{x_d}}{t} \quad (2)$$

where t denotes the test duration (s), Z the valence of chloride ion (Z = 1), F the Faraday constant (F = 96480 $J.V^{-1}.mol^{-1}$), ΔE the actual electrical potential drop between the two sides of the sample (V), R the ideal gas constant (R = 8.3144 $J.mol^{-1}.K^{-1}$), and T the absolute temperature (K). α is the auxiliary term defined in [45] as a function of the test conditions.
A test based on this principle has been standardized in the Nordic countries [46]. The COV of this test is equal at the maximum to 24% (resp. 15%) with regard to reproducibility (resp. repeatability) for every type of concretes according to [27] and [46].

Here, nss migration tests have been carried out after vacuum saturation of the samples (thickness: e = 50 ± 1 mm, and diameter 110 mm) with a 0.1 M NaOH solution. The samples are epoxy-coated around their cylindrical surface and mounted between the two compartments of a so-called migration cell [43,47]. The cell-sample interface is also coated with epoxy, in order to insure a watertight joint. The upstream compartment (catholyte) contains (0.5- or 1-M) NaCl + 0.1-M NaOH, while the initial downstream solution (anolyte) is 0.1-M NaOH. The volume of each compartment solution is 1 litre. An external potential drop is applied by electrodes at the sample boundaries and kept constant during the test. Its value has been restricted to 30 V. Depending on the mix-composition and on the potential drop value, the test lasted between 1 and a few days.

Results and discussion. The *apparent* chloride diffusion coefficient $D_{ns(mig)}$ (average values of three samples) measured according to the method described in the previous section on a large number of concretes after water curing and vacuum saturation is plotted *vs*. the average 28-day cylinder c.s. of the materials in Fig. 5. The L, M, H and VH classes, as previously defined, are reported in the graph. The associated thresholds between classes are 50, 10, 5 and 1, respectively [7]. The results obtained on the water-cured mortar samples are presented in Fig. 6. The values circled for a same 28-day c.s in Fig. 5 show the decrease in $D_{ns(mig)}$ when age increases (until 1 year) for a given concrete. Likewise, Fig. 6 shows the decrease in $D_{ns(mig)}$ when age increases in the case of the FA mortars. The decrease in $D_{ns(mig)}$ even after 1 year has been reported in the literature in the case of high-volume FA mortars with similar W/B as tested here.

Fig. 5 clearly illustrates, for a same average 28-day c.s., the efficiency of SF, FA or GGBS in reducing the *apparent* chloride diffusion coefficient: a higher durability level (class) is reached for SCM materials, compared to plain OPC - CEM I mixtures with same average 28-day c.s.. For example, the presence of SF induces a shift from the H to VH class.

Furthermore, good consistence is obtained from a given age between the values measured, on the one hand, on the various CEM-III concretes and, on the other hand, on the various FA-concretes tested. With regard to $D_{ns(mig)}$, the effect of SCM is more significant with respect to that of W/B. For example, CEM III/A concretes with 28-day c.s. ranging from 40 to 75 MPa (*i.e.* W/B from 0.44 to 0.54) exhibit $D_{ns(mig)} = 2.4\text{-}3 \cdot 10^{-12}$ $m^2.s^{-1}$, and thus very similar coefficients within this W/B range. The values recorded for the mentioned FA- and GGBS-concretes are very close to that found for HPCs (see Fig. 5). In other words, the effect of W/B on $D_{ns(mig)}$ can be significantly mitigated in the presence of FA or GGBS.

Normal-strength FA concretes (from 20 to 35% FA per unit mass of binder) display a very low coefficient and a high "potential" durability. More precisely, concretes with 28-day c.s. around 50 MPa, same cement, and 20-30% FA exhibit $D_{ns(mig)} = 1.5\text{-}2.4 \cdot 10^{-12}$ $m^2.s^{-1}$ between 28 days and 1 year (see Fig. 5). The efficiency of FA to decrease $D_{ns(mig)}$ is also illustrated for the mortars in Fig. 6. The reduction in the chloride diffusion coefficient in saturated conditions, with the increase in the FA content, illustrated in Fig. 6, has also been widely reported in the literature for lab data [31,33,38,48,49] and also for field data [50-53], despite a porosity often higher in particular at early age (dilution effect) [17]. These findings result from the refinement of the pore structure previously explained (see a previous section). Moreover, the (*apparent*) chloride diffusion depends on the chemical and physical chloride interactions with the cement matrix, as well as on electrical interactions between the ions in the pore solution and on (C-S-H) pore surfaces (electrical double layer, see a previous section). The physical interactions vary with the pore solution composition. And according to the literature [31,49], the nature and quantity of cations in FA-materials increase the resistance to diffusion of chloride anions: the higher calcium, silicium and aluminate concentrations and the lower potassium concentration decrease chloride mobility. Nevertheless, as shown in Fig. 6, the FA efficiency is more marked after 180 days than after 90 days. In addition, the difference between the values obtained at 90 days and at 180 days is larger in the case of the FA-mortars compared to FA-0. Furthermore, as illustrated by the B50FA result in Fig. 5, 180 days can be too early to observe the beneficial effect (due to a significant amount of additional C-S-H) of the high FA content (39%) exceeding its detrimental effect (coarse, porous and heterogeneous microstructure). This is further pointed out when comparing B50FA and M50FA (20% FA) results. Same type of conclusion can be made when comparing results on CFA (35% FA) at 4 and 7 months (see Fig. 5). Above 30% cement replacement, the delay to record a significant beneficial FA effect on $D_{ns(mig)}$ seems long. This is consistent with the optimum value (30%) found in the literature [54].

CEM III/A or CEM III/C concretes display a high "potential" durability for more or less similar reasons as FA-materials. This is in agreement with the literature, where it is reported that chloride diffusion in GGBS concretes is much slower than in CEM-I materials and even than in 30%-FA materials, as a result of the high tortuosity of the pore system and of chemical interactions between aluminates and chlorides (see a previous section and [55-57]).

No systematic effect of the presence of AEA is recorded on the *apparent* chloride diffusion coefficient, since diffusion (in saturated conditions) is limited by the smallest pores, even if a macropore network exists.

Since $D_{ns(mig)}$ decreases as a function of the age and reaches very low values in GGBS or FA materials, the value for old materials can be more hardly determined with accuracy according to the resolution limit of the method (*i.e.* clear and accurate detection of x_d), and this is enforced by the darkness of high-volume GGBS materials [43]. Therefore, the evolution of $D_{ns(mig)}$ as a function of the age in the medium or long term can be more hardly quantified than that of the electrical resistivity (ρ' increases as a function of the age).

It is worth noting that for plain OPC - CEM I mixtures (with local aggregates) currently used in common bridges in various areas in France, the $D_{ns(mig)}$ values (28-day - 1 year) are 6-17·10^{-12} $m^2.s^{-1}$. For these mixtures, a medium or low "potential" durability is therefore obtained (see Fig. 5).

Fig. 5 shows that a large range of $D_{ns(mig)}$ values and different "potential" durabilities can be obtained for a same average 28-day c.s. (or W/B), depending on the mix-composition. This is a clear illustration of the consequences of the new trends of concrete mix-design and of the relevance and the usefulness of a performance-based approach for durability assessment of complex mixtures. Mechanical properties (and in particular W/B) are not sufficient to estimate the "potential" durability of a RC and to select the appropriate mixture that meets durability requirements. Only a performance approach based on a set of DIs can in particular account for the gain provided by SCMs (and further by the combination of SCMs).

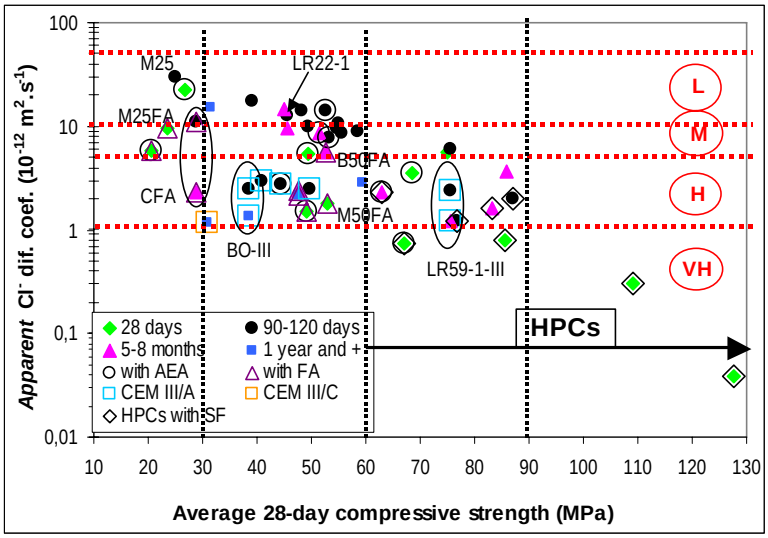

Fig. 5: "Potential" durability classes and experimental mean values of *apparent* chloride diffusion coefficient $D_{ns(mig)}$ measured by nss migration test under an external electrical field on saturated water-cured concrete samples at various ages *vs*. the average 28-day cylinder c.s..

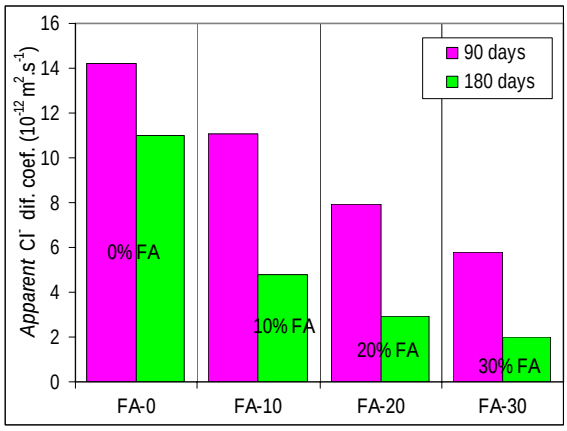

Fig. 6: Effect of the FA content on the *apparent* chloride diffusion coefficient $D_{ns(mig)}$ measured by nss migration test under an external electrical field on the saturated mortar samples (W/B = 0.45), after 90-day or 180-day water curing.

EFFECTIVE CHLORIDE DIFFUSION COEFFICIENT

Significance and methods of assessment. The *effective* chloride diffusion coefficient, which is the pure transport property (no binding effect) involved in *Fick's* first law or in *Nernst-Planck* equation, is an important parameter, since it is required for example as input data in predictive physical models of chloride ingress and more generally of ion transport [3,7,9]. It can be measured in saturated conditions directly by means of ss migration test. It could also be assessed by simple analytical formulas from parameters already measured in this paper: the electrical resistivity or the *apparent* chloride diffusion coefficient (see previous sections), which both involve an easier and quicker test, compared to ss migration.

Direct assessment of the *effective* chloride diffusion coefficient $D_{ss(mig)}$ from ss migration test. An *effective* chloride diffusion coefficient $D_{ss(mig)}$ can directly be assessed by a ss migration test from the monitoring of the chloride ion concentration *vs.* time by potentiometric titration in the downstream compartment of the migration cell where the concrete or mortar sample is tested. When the chloride flux and the potential drop at the boundaries of the sample are constant, $D_{ss(mig)}$ is provided by the modified *Nernst-Planck* equation, where the diffusion and advection flows are neglected with respect to the electrical migration one, and with the assumption of very dilute solutions and no interaction between ions in the pore solution (see Eq. (3)) [58,59]:

$$D_{ss(mig)} = \frac{R.T}{Z.F} \cdot \frac{e}{\Delta E} \cdot \frac{Q}{\gamma \cdot c_0 . t} \qquad (3)$$

where the chloride concentration of the catholyte solution (upstream compartment) c_0 is assumed to be a constant, γ is the activity coefficient of chloride ion in the catholyte solution and Q denotes the cumulative amount of chloride ions arriving in the downstream compartment during time t within the ss regime.
The constant chloride flux Q/t within the ss regime, required for the calculation, is assessed from the slope of the linear part of the plot giving the cumulative amount of chlorides *vs.* time.

Note that two other techniques can be used to assess $D_{ss(mig)}$ from ss migration test: conductivity measurement in the downstream compartment [62] or titration in the upstream compartment [63]. It was shown that the three techniques yield similar $D_{ss(mig)}$ results (see [3,8,64]). Nevertheless, it is worth noting that $D_{ss(mig)}$ measurement can suffer from poor accuracy in some cases as long as reproducibility is concerned: the COV was found equal to 76% with regard to reproducibility in the case of conductivity measurement, according to [27]. The value of 22% is reported in the same reference for the repeatability COV.

Ss migration tests have been carried out on 20-mm thick samples, according to [64], by using similar cells as that described for nss migration tests. Here, the upstream solution is 1-M NaCl + 0.1-M NaOH, while the initial downstream solution is 0.1-M NaOH. The actual potential drop between the surfaces of the sample is measured during the test by means of two reference electrodes contacting the sample surfaces.

Fig. 7 displays the *effective* chloride diffusion coefficients $D_{ss(mig)}$ (average values of three samples) directly assessed from ss migration tests by potentiometric titration in the downstream compartment *vs.* the average 28-day cylinder c.s.. The classes of "potential" durability L, M, H and VH, as previously defined, are also reported in the graph. The associated thresholds between classes are 8, 2, 1 and 0.1, respectively [7]. Again, normal-strength FA- or GGBS-mixtures are revealed out of the range obtained with plain OPC -

CEM I materials (*i.e.* significantly lower $D_{ss(mig)}$ values), except in the case of B50FA (age = 4 months) (see a previous section).

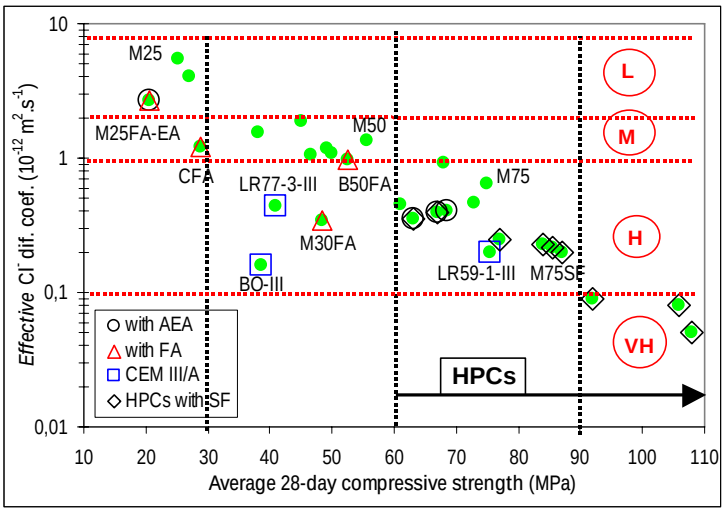

Fig. 7: "Potential" durability classes and experimental mean values of *effective* chloride diffusion coefficient $D_{ss(mig)}$ measured by ss migration test under an external electrical field on saturated concrete samples (90-day to 1-year water curing) *vs.* the average 28-day cylinder c.s..

Assessment of the *effective* chloride diffusion coefficient from nss diffusion test ($D_{eff(dif)}$) or from nss migration test ($D_{eff(mig)}$). Theoretical or simplified relationships exist between the *apparent* and the *effective* coefficients assessed by means of diffusion or migration tests, in particular by taking into account the chloride binding with the matrix. These relationships enable to deduce one of the coefficients from the other.

In the case of diffusion, when a constant binding capacity k_d is assumed (*i.e.* a linear binding isotherm), where k_d is the slope of the binding isotherm expressed here in mass by mass, the *effective* and *apparent* coefficients, $D_{eff(dif)}$ and $D_{ns(dif)}$ respectively, where $D_{ns(dif)}$ is directly measured by nss diffusion test [43,47,64], are linked by the following well-known Eq. (4):

$$D_{eff(dif)} = \Phi \cdot (1 + k_d) \cdot D_{ns(dif)} \quad (4)$$

Eq. (4) is not valid in the general case for migration. However, *Tang* demonstrated that a similar relationship could be written for migration tests, which involves the *apparent* coefficient $D_{ns(mig)}$ measured by nss migration test according to [46] and the constant "intrinsic" (*effective*) diffusion coefficient $D_{eff(mig)}$ [44,65]. Therefore, an *effective* chloride diffusion coefficient $D_{eff(mig)}$ can be calculated by means of a linear equation involving an *apparent* coefficient measured in nss conditions and a constant chloride binding capacity. Moreover, authors often assume that chloride binding can be neglected [61,66] or at least reduced [65] during nss migration tests. As a matter of fact, during nss migration tests, the velocity of the ions transported through the pore structure is very high and the contact time is short (usual test duration: 10-60h). This tends to impede adsorption and chemical reactions. Therefore, a very weak binding is expected, compared to diffusion (and also to ss migration), and binding may even be suppressed. A non-equilibrium state is expected and the hypothesis of instantaneous binding hence does not seem valid. *Castellote et al.* did point out a weak interaction in this kind of test, through fitting the experimental binding isotherm to a general BET equation (by assuming yet local equilibrium). These authors showed that equilibrium didn't seem to be achieved unless high amounts of NaCl (≥ 1 M) were used in the external solution [67]. Therefore, in a first approximation, the *effective* chloride diffusion coefficient

$D_{eff(mig)}$ can be deduced from the *apparent* chloride diffusion coefficient $D_{ns(mig)}$ directly assessed by a nss migration test by applying a colorimetric method (see a previous section) and by assuming no binding ($k_d = 0$). In this case, $D_{eff(mig)}$ can be calculated by Eq. (5):

$$D_{eff(mig)} = D_{ns(mig)} \cdot \Phi \quad (5)$$

Assessment of the *effective* chloride diffusion coefficient $D_{eff(resistivity)}$ from electrical resistivity measurement. An *effective* chloride diffusion coefficient $D_{eff(resistivity)}$ can theoretically be calculated from an electrical resistivity measurement, by using the modified *Nernst-Einstein* equation (a particular case of the *Nernst-Planck* equation using electrolyte equivalent conductivity as the main parameter [58,68], see Eq. (6)), which can be derived in Eq. (7):

$$\frac{\sigma_0}{\sigma} = \frac{D_0}{D_{eff}} = F \quad (6)$$

$$D_{eff(resistivity)} = \frac{D_0}{\sigma_0} \cdot \frac{1}{\rho'} \quad (7)$$

where F is the so-called formation factor, D_0 is the free diffusion coefficient of chlorides in the pore solution, and D_{eff} is the *effective* chloride diffusion coefficient in the porous material. The *effective* chloride diffusion coefficient is thus inversely proportional to the electrical resistivity ρ' of the water-saturated material and the coefficient of proportionality is dependent of the ionic concentrations (of the pore solution).

σ_0 should be assessed for each material tested. σ_0 can be measured by chemical analysis after pore solution expression [36]. Nevertheless, this requires specialized equipment and the very small volume then extracted could induce errors in the determination of σ_0. Hence, in a first approximation, the value $\sigma_0 = 11.87\ \Omega^{-1}.m^{-1}$ currently assumed for alkaline solutions similar to pore solutions of cementitious materials will be adopted. Note that for alkaline solutions, the value $\sigma_0 = 13.5\ \Omega^{-1}.m^{-1}$ is also found in the literature. In the case of a 1-M NaCl alkaline solution, σ_0 can reach the value $14.5\ \Omega^{-1}.m^{-1}$ according to [69]. The value $D_0 = 1.484 \cdot 10^{-9}\ m^2.s^{-1}$ will be adopted for the free diffusion coefficient of chloride ions in a 1-M solution at 25 °C [39,70]. Note that, as a result of electrical interactions between ions [61], the measured values of D_0 depend on the chloride concentration and higher values can be found in the literature, such as $2.032 \cdot 10^{-9}\ m^2.s^{-1}$ [66] or $2.1 \cdot 10^{-9}\ m^2.s^{-1}$ [23]. By assuming $\sigma_0 = 11.87\ \Omega^{-1}.m^{-1}$ and $D_0 = 1.484 \cdot 10^{-9}\ m^2.s^{-1}$, Eq. (8) is obtained:

$$D_{eff(resistivity)} \approx \frac{125}{\rho'} \qquad (\text{in } 10^{-12}\ m^2.s^{-1}, \text{ when } \rho' \text{ is in } \Omega.m) \quad (8)$$

Note that Eq. (8) is quite similar to the formula proposed by *Andrade et al.* for 1-M NaCl external solutions [22].

According to the comments given in a previous section, Eq. (8) will not be valid for the plain OPC - CEM I concretes tested here above a given W/C. For concretes with W/C ≥ 0.45, the lower σ_0 values computed in [42], by using the ionic concentrations and the electrical charges of the various ions present in the solution, will be adopted: $\sigma_0 = 5.0\ \Omega^{-1}.m^{-1}$ (calculated with M25) for W/C ≈ 0.80, $\sigma_0 = 6.7\ \Omega^{-1}.m^{-1}$ (calculated with a concrete with W/C = 0.62) for W/C = 0.60-0.70, and $\sigma_0 = 9.8\ \Omega^{-1}.m^{-1}$ (calculated with M50) for W/C = 0.45-0.55. Note that these computed σ_0 values were checked by chemical analysis of synthetic solutions (see [42]). The following equations Eq. (9) to Eq. (11) can thus be deduced for OPC - CEM I concretes (or FA- concretes when FA have not reacted), where $D_{eff(resistivity)}$ is in $10^{-12}\ m^2.s^{-1}$ when ρ' is in $\Omega.m$):

$$D_{eff(resistivity)} \approx \frac{151}{\rho'} \quad \text{for W/C = 0.45-0.55} \quad (9)$$

$$D_{eff(resistivity)} \approx \frac{221}{\rho'} \quad \text{for W/C = 0.60-0.70} \quad (10)$$

$$D_{eff(resistivity)} \approx \frac{297}{\rho'} \quad \text{for W/C} \approx 0.80 \quad (11)$$

Eq. (8) will be considered as valid for the other concretes.

Likewise, Eq. (8) will be considered as valid for the mortars tested here (W/B = 0.45), except for the plain OPC - CEM I ones. In this last case, the average value between the results published on hcps with W/C = 0.50 (σ_0 = 3.1 $\Omega^{-1}.m^{-1}$ [41] and σ_0 = 2.0 $\Omega^{-1}.m^{-1}$ [69]) and the result obtained on concrete M50 (σ_0 = 9.8 $\Omega^{-1}.m^{-1}$) will be used, *i.e.* σ_0 = 6.2 $\Omega^{-1}.m^{-1}$, and the same D_0 value as previously defined will be used, yielding Eq. (12):

$$D_{eff(resistivity)} \approx \frac{239}{\rho'} \quad \text{for OPC - CEM I mortars with W/C = 0.45} \quad (12)$$

Comparison of methods - Results and discussion. The simple methods proposed from $D_{ns(mig)}$ (see Eq. (5)) or from resistivity measurement, described in the previous sections, are compared in Fig. 8. In order to investigate further the validity of these simple methods, the associated results have been compared to the *effective* chloride diffusion coefficient $D_{ss(mig)}$ directly measured by means of ss migration test (see Eq. (3)) and to $D_{eff(dif)}$ (see Eq. (4)), where $D_{ns(dif)}$ has been calculated from the profiles measured after a nss diffusion test (curve-fitting by the so-called error function "erf") and the constant binding capacity k_d has been obtained from the free and total chloride concentration profiles (see Fig. 9a for mortars FA-0 and FA-30 at 90 days, and [43,47,64]). This comparison is presented in Figs. 9b, 9c and 9d, for a broad range of materials. Note that the concretes compared in Figs. 9c and 9d don't have systematically the same age. Therefore, in the general case the performances of these concretes cannot be directly compared.

Fig. 8 highlights excellent agreement between the two simple methods within the broad range of materials investigated (from 25 to 87 MPa). This means that both nss migration test and resistivity measurement provide exactly the same *effective* chloride diffusion coefficients, provided that the effect of the pore solution on ρ' is taken into account. These results also indicate that it is not possible to find a single non-empirical formula (*i.e.* not obtained by curve fitting), which is valid within the whole range of materials, for the assessment of the *effective* diffusion coefficient from resistivity measurement. This observation is of importance, since the range of materials available for users is becoming now broader and broader. In addition, Fig. 9 points out that the results provided by the simple methods ($D_{eff(resistivity)}$ and $D_{eff(mig)} = D_{ns(mig)} \cdot \Phi$) are in agreement with the results provided by direct measurement ($D_{ss(mig)}$) and with $D_{eff(dif)}$ (when available) ; the differences recorded are quite acceptable with respect to the precision of the test methods. The good agreement observed between $D_{eff(mig)} = D_{ns(mig)} \cdot \Phi$ and the other results confirms that very limited binding occurs during nss migration tests and that the assumption of no interaction is acceptable. These results indicate in addition that the assessment of the average chloride penetration depth (x_d) by $AgNO_3$ spray test is accurate enough, even in the case of the SCM-concretes tested here.

The assessment *via* nss diffusion test is more difficult than the other methods. As a matter of fact, the test is significantly longer, more laborious and more expensive. Moreover, ageing and other chemical effects can affect the results [3,47]. In particular, in the case of concretes with SCMs (more precisely FA), the test can only be used with old enough materials.

Otherwise, as a result of the evolving feature of these materials in the medium term and of the length of the test, $D_{ns(dif)}$ will correspond to a range of ages. Furthermore, the slope of the binding isotherm (k_d) has to be calculated from the experimental data for each material by the profile method [64] and this requires the assessment of both the total and the free chloride concentration profiles. Nevertheless, very similar values, whatever the material, have been found here for the coefficient $\Phi \cdot (1+k_d)$. This means that k_d decreases when Φ increases, confirming thereby that k_d is related to the C-S-H content of the material and quantifies mainly physical adsorption on C-S-H, as indicated in [44,65]. A mean value of 0.16 has been calculated here for the range of materials tested. Therefore, a simpler method can be proposed for the assessment of $D_{eff(dif)}$. It consists in measuring one of the chloride concentration profiles (free or total), then assessing the *apparent* coefficient $D_{ns(dif)}$ from it, and using the average fixed value 0.16 to calculate the coefficient $\Phi \cdot (1+k_d)$ and hence the *effective* chloride diffusion coefficient. Such calculations have been carried out here when experimental values were not available (see hachured bars in Fig. 9). As illustrated in Fig. 9, good agreement is observed between these results and the other methods, thus validating this simplified method based on nss diffusion test.

Whatever the method, the class of "potential" durability is the same, except of course when the results are very close to a limit between classes. In the general case, the values obtained, whatever the method when the age is higher than 90 days with HPCs, GGBS- and FA-concretes are very small (high or very high "potential" durability), illustrating again the efficiency of such concretes in reducing chloride transport. In the case of CFA (35% FA), FA are not sufficiently beneficial at 1-4 months and a medium "potential" durability is obtained (see Fig. 9c). On the other hand, at 4-7 months, the significant efficiency explains the high "potential" durability recorded (see Fig. 9d). Moreover, concretes BO-VB, BO-I and M50, with similar mix-compositions (in particular W/C), display similar *effective* chloride diffusion coefficients. Fig. 8 points out that D_{eff} of mortar FA-0 (W/C = 0.45) is higher than D_{eff} of plain OPC - CEM I concretes with W/C = 0.48-0.49 at 90 days (see e.g. M50, B50, and LR63-1-EA), confirming that, despite the possible improvement of the mortar matrix by the presence of limestone filler, a lower coefficient is found for concretes compared to mortars, as usually reported in the literature.

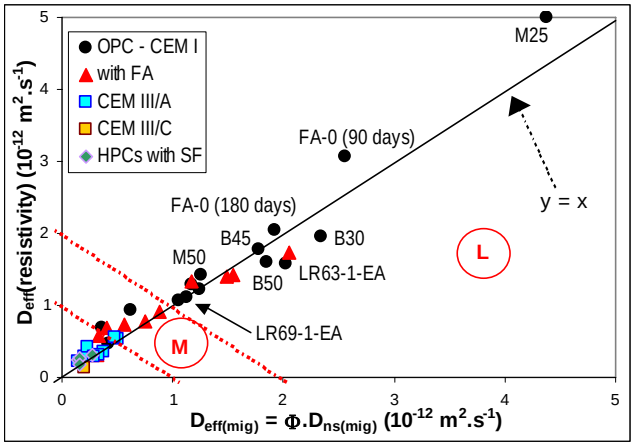

Fig. 8: Comparison between the *effective* chloride diffusion coefficients obtained from nss migration tests and from electrical resistivity, on saturated samples of various water-cured concretes and mortars. "Potential" durability classes.

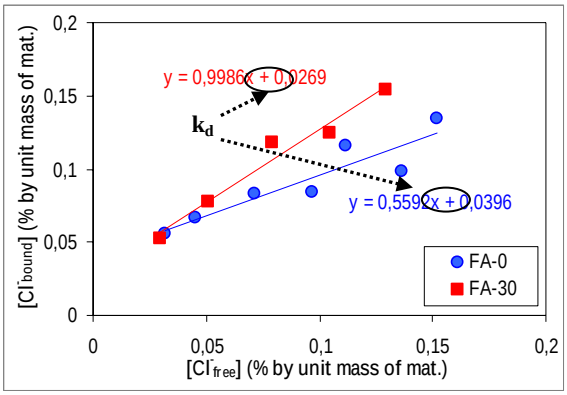

a) method of assessment of k_d from concentration profiles. Illustration with mortars FA-0 and FA-30 at 90 days

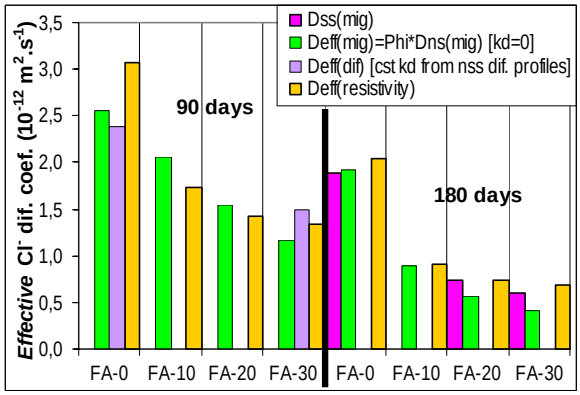

b) mortars with various FA contents (W/B = 0.45)

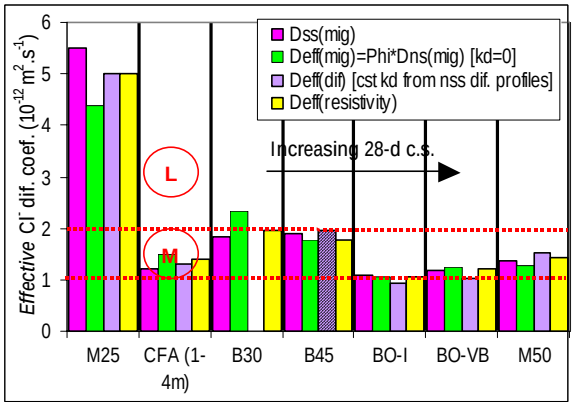

c) concretes with $D_{eff} \geq 1$ (L & M classes, according to [7])

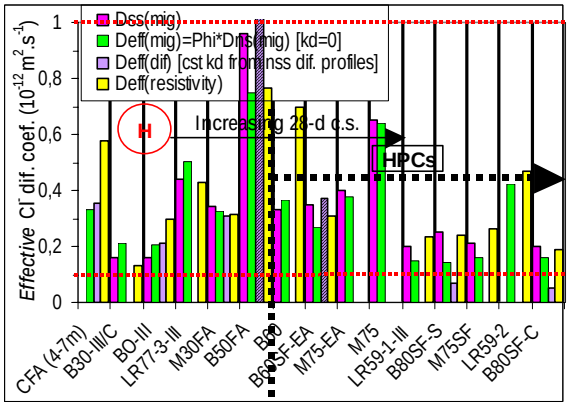

d) concretes with $D_{eff} < 1$ (H & VH classes, according to [7])

Fig. 9: *Effective* chloride diffusion coefficient obtained from ss or nss migration tests, from nss diffusion tests, and from electrical resistivity, on saturated samples, after various water curing periods. "Potential" durability classes.
hachured bars: $D_{eff(dif)} = 0.16 \cdot D_{ns(dif)}$

LIQUID WATER PERMEABILITY

Definition and significance. Among the transport properties, the liquid water permeability $k_l.k_{rl}(s)$ of a non-saturated medium, where s is the degree of liquid water saturation, k_l the permeability of the saturated material (*i.e.* at s = 1) and k_{rl} the relative permeability to liquid (k_{rl} = 1 at s = 1), governs the (advective) transport of liquid water according to the extended *Darcy's* law. This law characterizes the viscous flow of an incompressible and non-reactive fluid under a total pressure gradient and reads in a one-dimensional scheme along a Ox-axis (see Eq. (13)):

$$v_l = -\frac{k_l}{\eta_l} \cdot k_{rl}(s) \cdot \frac{\partial p_l}{\partial x} \qquad (13)$$

where v_l denotes the filtration velocity of liquid water, η_l its dynamic viscosity, and p_l the liquid pressure.
The permeability $k_l.k_{rl}(s)$ thus depends on the characteristics of the fluid, on the pore network (pore sizes, connectivity, tortuosity, …) and on other voids (microcracks, paste-aggregate interfacial zone, ...) of the material, as well as on the moisture state of the sample.

This parameter is of major practical interest even with respect to the protection against chloride-induced reinforcement corrosion. As a matter of fact, chloride ingress in tidal zones is very dependent on the liquid permeability of the material and not only on its chloride diffusion coefficient (see [9]). Hence, k_l is required as input data in physical moisture or coupled transport models [9,42,71].

Assessment of the liquid water permeability k_l by *Katz-Thompson* relationship - Results and discussion. It is widely admitted that the direct measurement of k_l in the case of low-permeability materials is difficult [7,72,73] and requires advanced experimental devices (see e.g. [74,75]). With regard to indirect methods, an important work on this topic has been performed by *Scherer* (e.g. rapid methods such as beam bending or thermopermeametry, first applied to gels and later extended to more rigid materials and recently to cement pastes [76]).

According to the literature, for some kinds of materials, k_l could be estimated by the *Katz-Thompson* relationship (see Eq. (14)), originally developed for sedimentary rocks and based upon the percolation theory [77,78], when the critical (*i.e.* breakthrough) pore diameter d_c and the formation factor F (see Eq. (6)) of the material are known [39,73,79-82]:

$$k_l = \frac{d_c^2}{226 \cdot F} \quad (14)$$

However, Eq. (14), which is a relationship between pore network parameters and transport property, can be considered as validated only for normal-strength materials, and more particularly for hardened cement pastes [76].

Katz-Thompson relationship has been applied here to various mortars and concretes at various ages. In Figs. 10a and 10b are compared the values of k_l obtained by Eq. (14) when F is calculated, on the one hand, as the ratio of *effective* chloride diffusion coefficients, and on the other hand, as the ratio of electrical conductivities. The *effective* chloride diffusion coefficient has been directly assessed by Eq. (3) (ss migration test) or by Eq. (5) (nss migration test and porosity) when ss migration test data were not available. The critical pore diameter d_c has been assessed from MIP measurement: d_c is associated with the sudden change in slope observed on the pore volume *vs.* diameter curve. As illustrated in Figs. 10a and 10b, very good agreement is observed between the k_l values assessed by the two methods of calculation of F, as theoretically expected, thus emphasizing the appropriate accuracy of both types of measurement. Fig. 10b emphasizes that portland cement replacement by 10 to 30% FA is not efficient to decrease the liquid water permeability at 90 days, contrary to the observations made with $D_{ns(mig)}$ (see Fig. 6). Likewise, *Hedegaard* in 1992 [83] showed by direct measurement the weak efficiency of FA at 28 and 56 days to reduce the liquid water permeability (a single FA was tested). Conversely, the beneficial effect on k_l at 180 days is obvious (see Fig. 10b) and is in agreement with the literature (direct measurement [38]). This results from the fact that the decrease in the void volume and the increase in the tortuosity, due to the incorporation of SCM, affect first the zones around C-S-H clusters (outer products) and at the paste-aggregate interface. Therefore, k_l will be significantly affected only when the larger-size (e.g. capillary) void network will be disconnected. On the other hand, the diffusion coefficient is affected as soon as the C-S-H gel pore network is disconnected. Contrary to Fig. 8 (D_{eff}), Fig. 10 points out the efficiency of the FA-0 mortar matrix to decrease k_l: the value is lower than the values recorded for plain OPC - CEM I concretes even with lower W/C (see e.g. B55 (W/C = 0.41) and LR69-1-EA (W/C = 0.43)).

Fig. 11 depicts the values of k_l (mean values of the two methods of calculation of F, except for LR22-1 where no resistivity value was available) assessed by *Katz-Thompson* relationship *vs*. the average 28-day cylinder c.s.. Fig. 11 exhibits the range of k_l values obtained when the

28-day c.s. of the materials ranges from 25 to 87 MPa. Whatever the age (≥ 90 days), normal-strength GGBS-concretes are revealed almost as efficient as SF-HPCs to reach very low liquid water permeabilities. These k_l values are at least one order of magnitude lower than that of plain OPC - CEM I with same c.s..

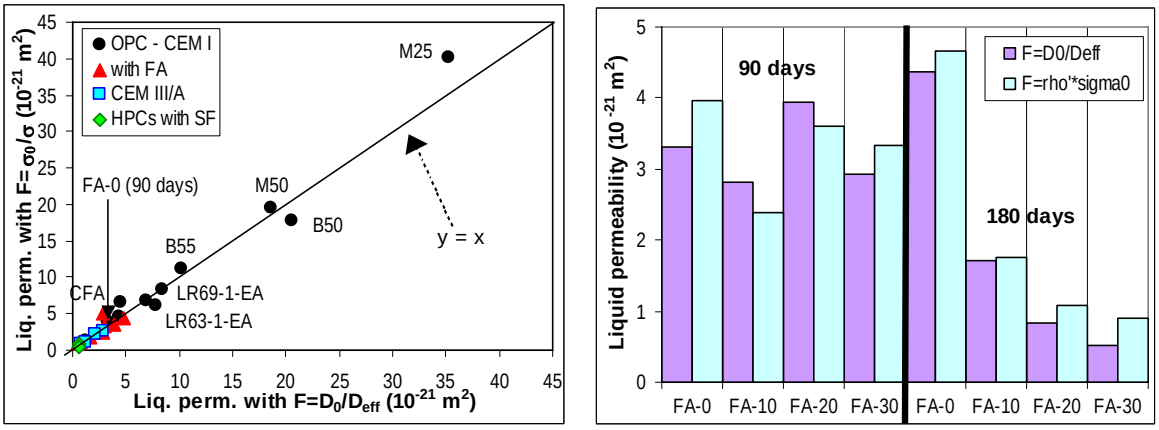

a) various concretes and mortars, at various ages

b) mortars (W/B = 0.45 and various FA contents), after 90-day or 180-day water curing

Fig. 10: Comparison between two methods of calculation of the liquid water permeability of saturated materials (k_l) by using *Katz-Thompson* relationship.

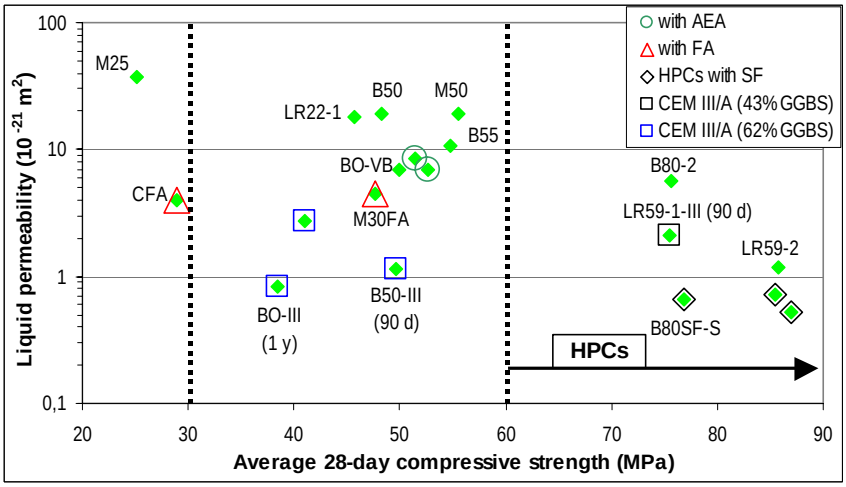

Fig. 11: Mean values of liquid water permeability of saturated concretes (k_l) assessed by *Katz-Thompson* relationship *vs.* the average 28-day cylinder c.s..

Assessment of liquid water permeability k_l by numerical inverse analysis - Comparison with *Katz-Thompson* relationship. In order to test the validity of the empirical *Katz-Thompson* method to assess the liquid water permeability k_l of concretes, a comparison has been carried out with a more sophisticated but more theoretical method. This is an indirect method (based on inverse analysis), which combines experiments and numerical model. This method, initially proposed by *Coussy et al.* [84], is based on the analysis of the relative mass loss *vs.* time plot (kinetics), associated with a drying test at a given relative humidity (RH) and at constant temperature (see the description of the experiments and computations in [47] and [85]). It requires an advanced isothermal moisture transport model, which involves the transport of liquid water and gas according to the extended *Darcy's* law and the relative diffusion of water vapour with respect to gas mixture governed by *Fick's* first law, with non-

constant total gas pressure [71]. In addition, this method requires the assessment of a few basic material properties ; the porosity, the gas permeability and the water vapour desorption isotherm [85] of the material are the other main inputs of the model. Moreover, the initial moisture state has to be known. It usually corresponds to almost saturated conditions ($s \approx 1$). k_l is hence deduced from the best fitting of the predicted drying kinetics by the model on the values observed for the sample submitted to the drying test (e.g. exposure to RH = 54% for 6 months, see Fig. 12a).

This method has been applied here to different types of concretes. The results obtained are compared in Fig. 12b to the results obtained by *Katz-Thompson* relationship (see previous section). In this last case, the value used for the formation factor F is the average between the ratio of electrical conductivities and the ratio of *effective* chloride diffusion coefficients. Fig. 12b points out that the results provided by the simple empirical method are quite consistent with the theoretical computations (inverse analysis) based on completely different tests for the various types of concretes tested. This confirms the relevance and the validity of *Katz-Thompson* relationship to assess the permeability of concretes, even in the presence of SCMs. Of course, in order to further validate the method, comparison with direct permeability measurement should be made. Note that, when the mentioned numerical model (or a simplified one [84]) and the required input data are available, the method based on inverse analysis has also the advantage of requiring a single simple experiment, which does not need any specific apparatus and which can be carried out easily in every lab.

M30FA (30% FA) and BO-III (62% GGBS) have been tested here at the same age (1 year) and have the same W/B. But despite its lower 28-day c.s. (see Table 1), BO-III exhibits a lower k_l value than M30FA (30% FA).

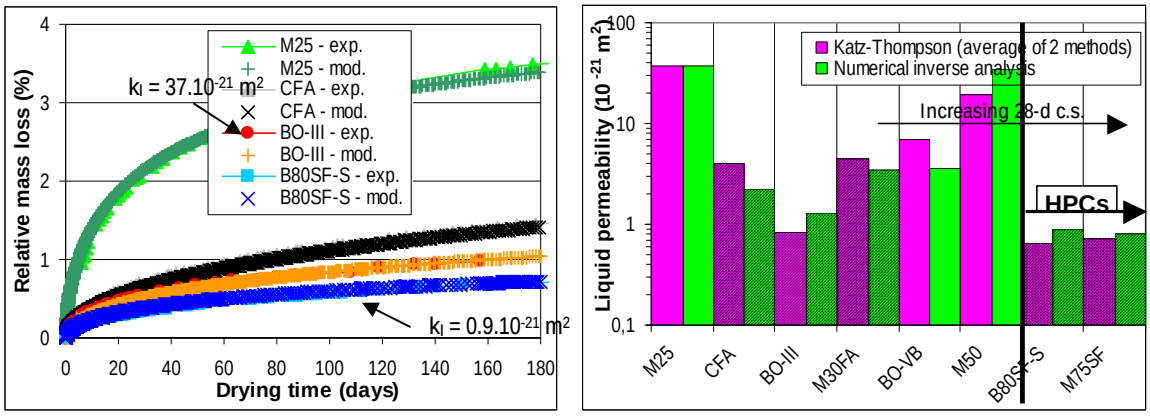

a) method of assessment: fitting of drying kinetics of samples submitted to RH = 54% and to T = 21 ± 1 °C for 6 months after 1- or 2- year water curing and saturation.

b) comparison with *Katz-Thompson* relationship. *SCM-concretes are hachured.*

Fig. 12: Liquid water permeability of saturated concretes (k_l) assessed by numerical inverse analysis from drying kinetics.

CONCLUSION

Very different methods for assessing, on the one hand the *effective* chloride diffusion coefficient, and on the other hand the liquid water permeability k_l, of saturated materials have been compared in this paper on a set of water-cured concretes ranging from low-grade to high-performance materials. The very good agreement observed in each case points out the validity and the reliability of the proposed methods. More precisely, the *effective* chloride

diffusion coefficient can be assessed from resistivity measurement, nss migration test, ss migration test and nss diffusion test. Likewise, k_l can be assessed from the *Katz-Thompson* relationship, as well as from numerical inverse analysis from drying kinetics. Resistivity measurement is not very discriminating for high-porosity plain OPC - CEM I concretes. Difficulties can also be exhibited in nss migration (or diffusion) tests with dense or high-volume GGBS concretes. Nevertheless, simple and rapid test methods can allow assessment of DIs with sufficient accuracy in the general case. An advanced statistically-based investigation of the precision of the lab tests for a broad range of materials remains to be done, as well as direct measurement of liquid permeability, in order to achieve the evaluation of the methods.

The specificities of the behaviour of SCM mixtures have been pointed out. As expected, good durability-related properties have been pointed out for mature concretes mixed with CEM III/A (43% or 62% GGBS) or with FA (20 to 35%). The transport properties (*apparent* and *effective* chloride diffusion coefficients, as well as liquid permeability) of such normal-strength concretes can be close to that of HPCs with SF, even if the porosity is not very low. Nevertheless, the results have also enhanced the higher and determining ageing effect associated with these materials (more marked with FA), and this is emphasized in the case of k_l. As a matter of fact, significantly better properties are recorded at later ages, after water curing, within the range investigated here and hence very different DI values can be measured, depending on the age. For example with the mortars tested here (10 to 30% FA), even if the FA beneficial effect is exhibited on the *apparent* chloride diffusion coefficient from 90 days, FA are revealed as beneficial only at 180 days with regard to k_l. This confirms the usefulness and the complementarity of these two DIs to assess the "potential" durability related to reinforcement corrosion. Only a performance approach based on a set of DIs can in particular account for the gain provided by SCMs. Furthermore, no improvement has been recorded on the *apparent* and *effective* chloride diffusion coefficients for the 39%-FA concrete tested here even at 180 days.

In field conditions, the beneficial effect of FA or GGBS will be mitigated (as a result of early-age drying, early exposure to aggressive species, carbonation, skin effect, ...) and will markedly depend on the curing and environmental conditions, since such SCM-materials (in particular FA) are very sensitive to these conditions. This has been illustrated for example within the framework of the BHP 2000 French National Project [15] in the study carried out both in lab and in various outdoor environments on some of the concretes investigated here. Therefore, it is particularly important to investigate the long-term behaviour both in lab and in field conditions in the case of concretes with high volume of SCM. More precisely, first it is of importance to perform lab tests at 90 days and even at 180 days, on the one hand to characterize the bulk concrete properties, and on the other hand to avoid errors and variability associated with lab tests due to ageing effects. In addition, it is necessary to account for early-age behaviour, which will characterize the "covercrete" of the structure.

The methods and the corresponding results on various types of materials presented in this paper can be useful to assist engineers in selecting a reliable methodology to assess DIs and carry out durability evaluation or prediction. In particular, the database displayed in the paper can provide helpful references when testing new materials or searching to meet durability criteria. The values can also be used as input data in predictive models for similar mixtures as those tested in this study, thus allowing to avoid long lab tests before implementation of the model. A performance-based approach along with the simple methods discussed here to assess the DIs can constitute a useful tool to address the durability of new materials within

the framework of sustainable development. This will contribute to the development of new high-tech and green solutions.

ACKNOWLEDGEMENTS

The authors gratefully acknowledge P. Belin, J.F. Bouteloup, L. Routhe and Xaomeng Wang (LCPC, Paris, France), as well as the LRPCs of Clermont-Ferrand (B. Boulet), Est Parisien (C. Mallet), Lille (J.J. Brioist), Lyon (M. Dierkens), and Saint-Brieuc (B. Thauvin), for their contribution to the experiments and their involvement in the LPC research project *"Performance-based and probabilistic durability approach"*.

REFERENCES

[1] Aïtcin P.C., Cement and concrete development from an environmental perspective, Proc. Int. Workshop "Concrete Technology for a sustainable development in the 21st century", june 1998, Lofoten Islands, Norway.

[2] Lukasik J., Damtoft J.S., Herfort D., Sorrentino D., Gartner E.M., Sustainable development and climate changes initiatives, Proc. 12th Int. Congress on the Chemistry of cement (ICCC 2007), july 8-13, 2007, Montréal, Québec, Canada (Ed. by J.J. Beaudoin, J. Makar & L. Raki, Montréal, 2007).

[3] Baroghel-Bouny V., Development of a global, performance and predictive approach of durability of (reinforced) concrete structures on the basis of durability indicators - Results and perspectives. Characterization of the microstructure of concretes, study of their moisture and transport properties, assessment of free deformations and service life prediction (in French), Etudes et Recherches des LPC, OA 63 (LCPC, Paris, 2008), 311 p.

[4] Leboullenger B., Account for global cost in the construction field in public policies. Methodological considerations (in French), Proc. AFGC Technical Seminar "Cycle de vie des ouvrages : une approche globale (GC'2009)", 18-19 march 2009, Cachan, France.

[5] FIB 2006 - Model Code for Service Life Design, FIB Bulletin 34 (2006) 110 p.

[6] CEN Technical Report - Guidance on the EN 206 equivalent durability procedure, CEN/TC104/SC1/TG17 Working draft, oct. 2009.

[7] Baroghel-Bouny V. *et al.*, Concrete design for a given structure service life - Durability management with regard to reinforcement corrosion and alkali-silica reaction. State-of-the-art and guide for the implementation of a predictive performance approach based upon durability indicators, AFGC Scientific and Technical Documents (AFGC, Paris, issue in French: 2004, issue in English: 2007), 240 p.

[8] Baroghel-Bouny V., Durability indicators: relevant tools for an improved assessment of RC durability, Proc. 5th Int. Conf. on Concrete under severe conditions: Environment and loading (CONSEC'07), june 4-6, 2007, Tours, France (Ed. by F. Toutlemonde, K. Sakai, O.E. Gjørv & N. Banthia, LCPC, 2007), vol. 1, 67-84.

[9] Baroghel-Bouny V., Nguyen T.Q., Dangla P., Assessment and prediction of RC structure service life by means of durability indicators and physical/chemical models, Cem. Conc. Comp. 31 (8) (2009) 522-534.

[10] Atkins M., Glasser F.P., Application of Portland cement-based materials to radioactive waste immobilisation, J. of Waste Management 12 (1992) 105-131.

[11] Thomas M.D.A., Shehata M.H., Shashiprakash S.G., Hopkins D.S., Cail K., Use of ternary cementitious systems containing silica fume and fly ash in concrete, Cem. Con. Res. 29 (1999) 1207-1214.

[12] Bilodeau A., Malhotra V.M., High-volume fly ash system: concrete solution for sustainable development, ACI Mat. Journ. 97 (1) (2000) 41-49.

[13] Bleszynski R., Hooton R.D., Thomas M.D.A., Rogers C.A., Durability of ternary blend concrete with silica fume and blast-furnace slag: laboratory and outdoor exposure site studies, ACI Mat. Journ. 99 (5) (2002) 499-508.

[14] Naik T.R., Ramme B.W., Kraus R.N., Durability of concrete with high-volumes of fly ash, Proc. Int. Seminar on Durability and lifecycle evaluation of concrete structures - 2004, sept. 13, 2004, Higashi-Hiroshima, Japan (Ed. by R. Sato, Y. Fujimoto & T. Dohi, Univ. of Hiroshima, 2004).
[15] Baroghel-Bouny V., Gawsewitch J., Belin P., Ounoughi K., Arnaud S., Olivier G., Bissonnette B., Ageing of concrete in natural environments: an experiment for the 21st century. IV - Results on cores extracted from field-exposed test specimens of various sites as part of the first measurement sequence, Bul. Lab. Ponts & Chaus. 249 (2004) 49-100.
[16] De Larrard F., Baroghel-Bouny V., Ageing of concrete in natural environments: an experiment for the 21st century. I - General considerations and initial mechanical properties of tested concrete (in French), Bul. Lab. Ponts & Chaus. (225) (2000) 51-65.
[17] Kinomura K., Baroghel-Bouny V., Pore Structure and transport properties of high-volume fly ash materials used for radioactive waste disposal facilities, Proc. Int. RILEM Workshop "Long-Term performance of cementitious barriers and reinforced concrete in nuclear power plants and waste management (NUCPERF 2009)", 30 march - 02 april 2009, Cadarache, France.
[18] "GranDuBé - Grandeurs associées à la durabilité des bétons (Durability-related parameters)" (in French) (Ed. by G. Arliguie & H. Hornain, RGCU - AFGC - Presses de l'ENPC, Paris, april 2007), 63-106.
[19] Andrade C., d'Andréa R., Electrical resistivity as microstructural parameter for the calculation of reinforcement service life, Proc. Int. Conf. on Microstructure related durability of cementitious composites, oct. 13-15, 2008, Nanjing, China.
[20] Polder R.B., Test methods for on site measurement of resistivity of concrete - A RILEM TC-154 technical recommendation, Cons. Build. Mat. 15 (2-3) (2001) 125-131.
[21] Frederiksen J.M., Sorensen H.E., Andersen A., Klinghoffer O., The effect of the W/C ratio on chloride transport into concrete. Immersion, migration and resistivity tests, HETEK Report n° 54 (Ed. by V. Frederiksen, Danish Road Directorate, Copenhagen, 1997).
[22] Andrade C., Alonso C., Arteaga A., Tanner P., Methodology based on the electrical resistivity for the calculation of reinforcement service life, L'industria italiana del cemento 764 (2001) 330-339.
[23] Kyi A.A., Batchelor B., An electrical conductivity method for measuring the effects of additives on effective diffusivities in portland cement pastes, Cem. Conc. Res. 24 (4) (1994) 752-764.
[24] Tuutti K., Corrosion of steel in concrete, Report 4.82, Swedish Cem. Conc. Res. Inst. (CBI), Stockholm, Sweden, 1982.
[25] Belin P., Baroghel-Bouny V., Measurement of electrical resistivity of saturated concrete: development of a test method (in French), Research Project 11B021 "Durability of reinforced concrete and of its constituents: control and performance-based approach", Research Report, may 2006, LCPC, 18 p + annexes.
[26] Newlands M.D., Jones M.R., Kandasami S., Harrison T.A., Sensitivity of electrode contact solutions and contact pressure in assessing electrical resistivity of concrete, Mat. Struct. 41 (4) (2008) 621-632.
[27] ChlorTest - EU funded research project G6RD-CT-2002-0085 "Resistance of concrete to chloride ingress - From laboratory tests to in-field performance", WP 5 Report - Final evaluation of the test methods, prepared by Tang Luping, Deliverables D16-19, 2005, 38 p.
[28] Castellote M., Andrade C., Round-Robin Test on methods for determining chloride transport parameters in concrete, RILEM Technical Committee, Mat. Struct. 39 (10) (2006) 955-990.
[29] Larbi J.A., Fraay A.L.A., Bijen J.M., The chemistry of the pore fluid of silica fume-blended cement systems, Cem. Conc. Res. 20 (1990) 506-516.
[30] Richardson I.G., The nature of C-S-H in hardened cements, Cem. Conc. Res. 29 (1999) 1131-1147.
[31] Li S., Roy D.M., Investigation of relations between porosity, pore structure, and Cl^- diffusion of fly ash and blended cement pastes, Cem. Conc. Res. 16 (1986) 749-759.
[32] Villain G., Baroghel-Bouny V., Kounkou C., Comparative study of the induced hydration, drying and deformations of self-compacting and ordinary mortars, Proc. 1st Int. RILEM Symp. "Self-compacting concrete", sept. 13-17, 1999, Stockholm, Sweden (Ed. by A. Skarendahl & O. Petersson, RILEM, Paris, 1999), PRO 7, 131-142.
[33] Ngala V.T., Page C.L., Parrott L.J., Yu S.W., Diffusion in cementitious materials: II. Further investigations of chloride and oxygen diffusion in well-cured OPC and OPC/30% PFA pastes, Cem. Conc. Res. 25 (4) (1995) 819-826.

[34] Zhang T., Gjørv O.E., Diffusion behavior of chloride ions in concrete, Cem. Conc. Res. 26 (6) (1996) 907-917.
[35] Amiri O., Aït-Mokhtar A., Dumargue P., Touchard G., Electrochemical modelling of chloride migration in cement based materials. Part I: Theoretical basis at microscopic scale, Electrochemical Acta 46 (2001) 1267-1275.
[36] Page C.L., Vennesland O., Pore solution composition and chloride binding capacity of silica-fume cement pastes, Mat. Struct. 16 (91) (1983) 19-25.
[37] Hornain H., Thuret B., Guedon-Dubied S., Le Roux A., Laporte F., Pigeon M., Martineau F., Influence of aggregates and mineral additives on the composition of the pore solution, Proc. 10th ICAARC, Melbourne, Australia, August 18-23, 1996 (Ed. by A. Shayan), 514-521.
[38] Hussain S.E., Rasheeduzzafar, Corrosion resistance performance of fly ash blended cement concrete, ACI Mat. Journ. 91 (3) (1994) 264-272.
[39] Garboczi E.J., Permeability, diffusivity and microstructural parameters: a critical review, Cem. Conc. Res. 20 (4) (1990) 591-601.
[40] Cabrera J.G., Ghoddoussi P., The influence of fly ash on the resistivity and rate of corrosion of reinforced concrete, Proc. 4th CANMET/ACI Int. Conf. on Concrete durability, Nice, France, 1994, SP-145, 229-244.
[41] Tumidajski P., Schumacher A., Perron S., Gu P., Beaudoin J., On the relationship between porosity and electrical resistivity in cementitious systems, Cem. Conc. Res. 26 (4) (1996) 539-544.
[42] Thiery M., Modelling of atmospheric carbonation of cementitious materials. Account for kinetic effects as well as microstructure and moisture changes (in French), Etudes et Recherches des LPC, OA 52 (LCPC, Paris, 2006), 337 p.
[43] Baroghel-Bouny V., Belin P., Maultzsch M., Henry D., $AgNO_3$ spray tests - Advantages, weaknesses, and various applications to quantify chloride ingress into concrete. Part 2: Non-steady-state migration tests and chloride diffusion coefficients, Mat. Struct. 40 (8) (2007) 783-799.
[44] Tang L., Chloride transport in concrete - Measurement and prediction, Ph.D. Thesis, Publ. P-96:6, Depart. of Building Materials, Chalmers Univ. of Technology, Göteborg, Sweden, 1996, 461 p.
[45] Tang L., Nilsson L.O., Rapid determination of the chloride diffusivity in concrete by applying an electrical field, ACI Mat. Journ. 89 (1) (1992) 49-53.
[46] NT Build 492: Nordtest method, Concrete, mortar and cement-based repair materials: Chloride migration coefficient from non-steady-state migration experiments, Espoo, Finland, 1999.
[47] Baroghel-Bouny V., Thiery M., Barberon F., Coussy O., Villain G., Assessment of transport properties of cementitious materials: a major challenge as regards durability?, Euro. Rev. Civil Eng. 11 (6) (2007) 671-696.
[48] Lu X., Application of the Nernst-Einstein equation to concrete, Cem. Conc. Res. 27 (2) (1997) 293-302.
[49] Papadakis V.G., Effect of supplementary cementing materials on concrete resistance against carbonation and chloride ingress, Cem. Conc. Res. 30 (2000) 291-299.
[50] Alexander M.G., Mackechnie J.R., Predictions of long-term chloride ingress from marine exposure trials, in "Materials science of concrete", Special vol.: "Ion and mass transport in cement-based materials" (Ed. by R.D. Hooton, M.D.A. Thomas, J. Marchand & J.J. Beaudoin, Series Ed. J.P. Skalny, Am. Ceram. Soc., Westerville, 2001) 281-291.
[51] Mohammed T.U., Yamaji T., Hamada H., Chloride diffusion, microstructure, and mineralogy of concrete after 15 years of exposure in tidal environment, ACI Mat. Journ. 99 (3) (2002) 256-263.
[52] Thomas M.D.A., Matthews J.D., Performance of pfa concrete in a marine environment - 10-year results, Cem. Conc. Comp. 26 (1) (2004) 5-20.
[53] Du Preez A.A., Alexander M.G., A site study of durability indexes for concrete in marine conditions, Mat. Struct. 37 (267) (2004) 146-154.
[54] Dhir R.K., Jones M.R., Development of chloride-resisting concrete using fly ash, Fuel 78 (1999) 137-142.
[55] Page C.L., Short N.R., El Tarras A., Diffusion of chloride ions in hardened cement paste, Cem. Conc. Res. 11 (1981) 395-406.

[56] Dhir R.K., El-Mohr M.A.K., Dyer T.D., Chloride binding in GGBS concrete, Cem. Conc. Res. 26 (12) (1996) 1767-1773.
[57] Luo R., Cai Y., Wang C., Huang X., Study of chloride binding and diffusion in GGBS concrete, Cem. Conc. Res. 33 (1) (2003) 1-7.
[58] Andrade C., Calculation of chloride diffusion coefficients in concrete from ionic migration measurements, Cem. Conc. Res. 23 (3) (1993) 724-742.
[59] Andrade C., Sanjuan M.A., Experimental procedure for the calculation of chloride diffusion coefficients in concrete from migration tests, Adv. Cem. Res. 6 (23) (1994) 127-134.
[60] Tang L., Concentration dependence of diffusion and migration of chloride ions. Part 2: Experimental evaluations, Cem. Conc. Res. 29 (1999) 1469-1474.
[61] Nguyen T.Q., Baroghel-Bouny V., Dangla P., Prediction of chloride ingress into saturated concrete on the basis of a multi-species model by numerical calculations, Comp. Conc. 3 (6) (2006) 401-422.
[62] Castellote M., Andrade C., Alonso C., Measurement of the steady and non-steady state chloride diffusion coefficients in a migration test by means of monitoring the conductivity in the anolyte chamber. Comparison with natural diffusion tests, Cem. Conc. Res. 31 (10) (2001) 1411-1420.
[63] Truc O., Ollivier J.P., Carcasses M., A new way for determining the chloride diffusion coefficient in concrete from steady state migration tests, Cem. Conc. Res. 30 (2) (2000) 217-226.
[64] Baroghel-Bouny V., Belin P., Castellote M., Rafaï N., Rougeau P., Yssorche-Cubaynes M.P., Which toolkit for durability evaluation as regards chloride ingress into concrete? Part I: Comparison between various methods for assessing the chloride diffusion coefficient of concrete in saturated conditions, Proc. 3rd Int. RILEM Workshop "Testing and modelling chloride ingress into concrete", sept. 9-10, 2002, Madrid, Spain (Ed. by C. Andrade & J. Kropp, RILEM Publ., Bagneux, 2004), PRO 38, 105-136.
[65] Tang L., Nilsson L.O., Ionic migration and its relation to diffusion, in "Materials science of concrete", Special vol.: "Ion and mass transport in cement-based materials" (Ed. by R.D. Hooton, M.D.A. Thomas, J. Marchand & J.J. Beaudoin, Series Ed. J.P. Skalny, Am. Ceram. Soc., Westerville, 2001), 81-96.
[66] Samson E., Marchand J., Snyder K.A., Calculation of ionic diffusion coefficients on the basis of migration test results, Mat. Struct. 36 (2003) 156-165.
[67] Castellote M., Andrade C., Alonso C., Chloride-binding isotherms in concrete submitted to non-steady-state migration experiments, Cem. Conc. Res. 29 (1999) 1799-1806.
[68] Dullien F.A.L., "Porous Media. Fluid Transport and Pore Structure", Academic Press (1979).
[69] Rajabipour F., Weiss J., Electrical conductivity of drying cement paste, Mat. Struct. 40 (12) (2007) 1143-1160.
[70] Tong L., Gjorv O.E., Chloride diffusivity based on migration testing, Cem. Conc. Res. 31 (2001) 973-982.
[71] Thiery M., Baroghel-Bouny V., Bourneton N., Villain G., Stefani C., Modelling of drying of concrete - Analysis of the different moisture transport modes (in French), Euro. Rev. Civil Eng. 11 (5) (2007) 541-577.
[72] Perraton D., Aïtcin P.C., Carles-Gibergues A., Permeability, as seen by the researcher, in "High Performance concrete - From material to structure" (Ed. by Y. Malier, E. & F.N. Spon, Chapman & Hall, Cambridge, UK, 1992) pp 252-275.
[73] Martys N.S., Survey of concrete transport properties and their measurement, NIST Report NISTIR 5592, 1995, 40 p.
[74] Hearn N., Mills R.H., A simple permeameter for water or gas flow, Cem. Conc. Res. 21 (2/3) (1991) 257-261.
[75] El-Dieb A.S., Hooton R.D., A high pressure triaxial cell with improved measurement sensitivity for saturated water permeability of high performance concrete, Cem. Conc. Res. 24 (5) (1994) 854-862.
[76] Scherer G.W., Valenza II J.J., Simmons G., New methods to measure liquid permeability in porous material, Cem. Conc. Res. 37 (3) (2007) 386-397.
[77] Katz A.J., Thompson A.H., Quantitative prediction of permeability in porous rock, Physical Review B, 34, (11) (1986) 8179-8181.
[78] Thompson A.H., Katz A.J., Krohn C.E., The microgeometry and transport properties of sedimentary rocks, Adv. Phys., 36 (5), 1987, pp 625-693.

[79] El-Dieb A.S., Hooton R.D., Evaluation of the Katz-Thompson model for estimating the water permeability of cement-based materials from mercury intrusion porosimetry data, Cem. Conc. Res. 24 (3) (1994) 443-455.
[80] Halamickova P., Detwiler R.J., Bentz D.P., Garboczi E.J., Water permeability and chloride ion diffusion in portland cement mortars: relationship to sand content and critical pore diameter, Cem. Conc. Res. 25 (4) (1995) 790-802.
[81] Christensen B.J., Mason T.O., Jennings H.M., Comparison of measured and calculated permeabilites for hardened cement pastes, Cem. Conc. Res. 26 (9) (1996) 1325-1334.
[82] Tumidajski P.J., Lin B., On the validity of the Katz-Thompson equation for permeabilities in concrete, Cem. Conc. Res. 28 (5) (1998) 643-647.
[83] Hedegaard S.E., Hansen T.C., Water permeability of fly ash concretes, Mat. Struct. 25 (1992) 381-387.
[84] Coussy O., Baroghel-Bouny V., Dangla P., Mainguy M., Assessment of the water permeability of concretes from their mass loss during drying (in French), Rev. Fran. Génie Civil 5 (2-3) (2001) 269-284.
[85] Baroghel-Bouny V., Water vapour sorption experiments on hardened cementitious materials. Part I: Essential tool for analysis of hygral behaviour and its relation to pore structure, Cem. Conc. Res. 37 (3) (2007) 414-437.